Escape from black hole analogs in materials: Type-II Weyl semimetals and generic edge states

Koji Hashimoto* and Yoshinori Matsuo†
Department of Physics, Osaka University, Toyonaka, Osaka 560-0043, Japan

(Received 26 December 2019; accepted 2 November 2020; published 17 November 2020)

Type-II Weyl semimetals are dictated by bulk excitations with tilted light cones, resembling the inside of black holes. We obtain generic boundary conditions for surface boundaries of the type-II Weyl semimetals near Weyl nodes, and show that for a certain boundary condition edge states can escape out of the "black hole" event horizon. This means that for realization of the material "black hole" by the type-II Weyl semimetals, a careful choice of the boundary condition is necessary.

DOI: 10.1103/PhysRevB.102.195128

I. INTRODUCTION

Among various interplay between condensed-matter physics and particle physics, recent advances in physics on Weyl semimetals (see [1] for a recent review) are of particular interest because of their uniqueness about relativistic nature of quasiparticle excitations. Study of Weyl fermions in the Weyl semimetals enlarges the common grounds of the two subjects, not only through the anomaly and topological nature of Weyl fermions leading to the bulk-edge correspondence [2–4], but also with relativistic properties of Weyl fermions.

An intriguing picture of the latter was proposed by Volovik and Zhang [5], concerning in particular type-II Weyl semimetals [6]. Type-II Weyl semimetals are defined by Weyl points associated with overtilted Weyl cones, and Ref. [5] clarified that they correspond to light cones allowing propagation only in a certain direction, which in particle physics typically appears behind event horizons of black holes. An analog of a wider region in the black hole geometry including both sides of the horizon, can be reached by inhomogeneous Weyl semimetals which have some surface of the transition between types I and II [5,7–11].

In this paper, we combine theoretically the idea [5] of equivalence between the type-II Weyl semimetals and black holes, and the bulk-edge correspondence. We analyze most generic edge dispersion of continuum type-II Weyl semimetals. The aim is to study whether the idea of identifying the type-II Weyl semimetals with the inside of the black holes is valid even with the presence of the edge modes. The edge modes have quite different behaviors from the particle propagation in vacuum. Despite the significance of the edge modes in topological material, the edge modes appear as extra degrees of freedom which do not resemble any propagating modes around real black holes in analogous models of black holes. In order to capture the analogous features to black holes, effects of the edge modes should be distinguished from the bulk modes. In particular, an important question is whether the edge modes can escape from the black hole. For example, if the edge mode can escape, the information of the bulk modes inside the horizon would also leak to the outside through interactions with the edge modes. At the same time, it may also provide an additional access to the information inside the horizon. If the edge mode cannot escape, it gives no additional outflow of the information. It is simply an unnatural mode which does not alter the information structure of the black hole analogs. Since more concrete approaches to emulate the global structure of the black hole geometry by inhomogeneous Weyl semimetals have been studied elsewhere, we will focus on local behaviors of the edge modes in a region which is identified with the inside of the black holes. We follow the strategy developed in Ref. [12] on all possible allowed boundary conditions in the continuum limit to seek for a possibility of escaping out of the "black hole." We find that for a certain class of the boundary conditions of the surface of the semimetal, edge modes can escape from the black hole. This means that the identification needs a proper choice of the boundary condition.

The organization of this paper is as follows. First, in Sec. II we briefly review continuum type-II Weyl semimetals and their relation to black holes. Then, in Sec. III we introduce generic boundary condition analysis for type-II Weyl semimetals with surfaces. In Sec. IV we explicitly calculate the generic edge dispersion of type-II Weyl semimetals. In Sec. V we provide a useful theorem that any edge dispersion is tangential to and ending at bulk dispersion, for generic Weyl semimetals. Then, finally, in Sec. VI we calculate space-time light-cone structure for the edge modes and find that they can escape from the black hole for a choice of the surface boundary conditions. The final section is for a summary and discussions.

II. TYPE-II WEYL SEMIMETALS AND BLACK HOLES

Let us briefly review the relation between the type-II Weyl semimetals and light-cone structure [5,7]. We consider a three-dimensional Weyl semimetal in the continuum limit,

*koji@phys.sci.osaka-u.ac.jp
†matsuo@het.phys.sci.osaka-u.ac.jp

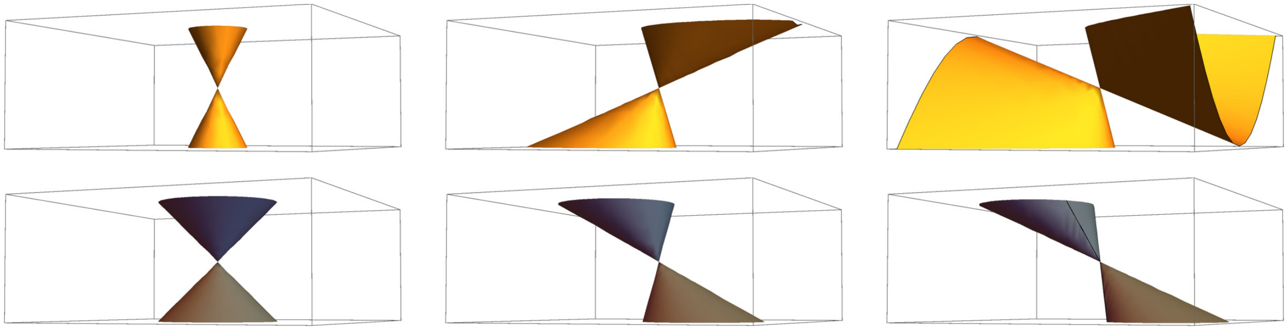

FIG. 1. Upper row: energy dispersion E_{bulk} as a function of p_1 and p_2 at the slice $p_3 = 0$. For simplicity we choose $\alpha_2 = \alpha_3 = 0$, with $\alpha_1 = 0$ (left, type I), $\alpha_1 = -0.8$ (middle, type I), $\alpha_1 = -1.2$ (right, type II), respectively. Lower row: Corresponding light cones. It is seen that the type-II dispersion (right) has a large tilt of the light cone such that it allows only a propagation to the negative direction of x^1.

whose Hamiltonian is given by

$$H = p_i\sigma_i + \alpha_i p_i \mathbf{1}, \tag{1}$$

where the summation is made for $i = 1, 2, 3$ and σ_i are the Pauli matrices. This Hamiltonian is general enough to capture the topological charge of the Weyl semimetal, chirality $= +1$, after a proper redefinition of the momentum axis and its normalization. The parameters α_i $(i = 1, 2, 3)$ are real constants.[1]

The bulk dispersion which follows from (1) is

$$E_{\mathrm{bulk}} = \alpha_i p_i \pm \sqrt{(p_i)^2}. \tag{2}$$

For $(\alpha_i)^2 > 1$, the bulk dispersion at $E = 0$ is not a single point, but forms a set of flat surfaces in the momentum space, which defines the type-II Weyl semimetals (see Fig. 1).

Let us derive the light-cone structure of the propagation of the excitation from the dispersion relation (2). It can be recast to the form $g^{\mu\nu} p_\mu p_\nu = 0$ with the effective metric

$$g_{\mu\nu} = \begin{pmatrix} 1-\alpha_i^2 & \alpha_1 & \alpha_2 & \alpha_3 \\ \alpha_1 & -1 & 0 & 0 \\ \alpha_2 & 0 & -1 & 0 \\ \alpha_3 & 0 & 0 & -1 \end{pmatrix}_{\mu\nu} \tag{3}$$

with the standard identification $p_0 = -E$ (to make sure that the wave function is written as $\exp[-iEt + ip_i x^i]$).

In the following we show in two ways that this is the metric inside of a black hole. First, consider a Schwarzschild black hole metric in Painlevé-Gullstrand coordinates

$$ds^2 = \left(1-\frac{2M}{r}\right)dt^2 - 2\sqrt{\frac{2M}{r^3}}dt\, x^i dx^i - (dx^i)^2, \tag{4}$$

where $r^2 = (x^i)^2$. The horizon is at $r = 2M$. This metric reproduces (3) under the identification

$$\alpha_i = -\sqrt{\frac{2M}{r^3}}x^i. \tag{5}$$

So, the Weyl semimetal is a local description in the geometry of the Schwarzschild black hole. It is only for phenomena in the vicinity of a point defined by (5) because α_i depends on the position in the Schwarzschild metric, but is a constant for the Weyl semimetal. The parameter α_i is now related to the radius in the Schwarzschild metric at the point which the Weyl semimetal mimics, as $(\alpha_i)^2 = 2M/r$. If it is identified with a point inside the black hole, $r < 2M$, then $(\alpha_i)^2 > 1$, so it corresponds to the dispersion of the type-II Weyl semimetal. An analog in a wider region with x dependent α can be reached by inhomogeneous Weyl semimetals. We focus on a region near the horizon $r \simeq 2M$. We define $x^i = x_0^i + \delta x^i$ and take $r_0 = \sqrt{(x_0^i)^2} \simeq 2M$. Then, (5) is expanded as

$$\alpha_i = -\sqrt{\frac{2M}{r_0}}\mathbf{e}^i + \delta\alpha_i(x), \tag{6}$$

where $\mathbf{e}^i = x_0^i/r_0$ and the correction term $\delta\alpha_i(x)$ is expressed as[2]

$$\delta\alpha_i(x) = -\sqrt{\frac{2M}{r_0^3}}\left(\delta x^i - \frac{3}{2}\mathbf{e}^i\mathbf{e}^j\delta x^j\right) + \cdots. \tag{7}$$

We can take the size of the region L, where $-L < \delta x^i < L$, for example, to be much smaller than the Schwarzschild radius since the wavelength of the wave function should be much shorter than the size of black holes. Then, the correction terms with x dependence will be sufficiently small

$$\delta\alpha_i(x) \sim \frac{L}{2M} \tag{8}$$

and, hence, can be resembled by inhomogeneous Weyl semimetals. Although inhomogeneous Weyl semimetals have

[1]Since the Hamiltonian (1) is the low-energy approximation, in reality there exist higher-order terms in momenta. However, inclusion of those higher-order terms will spoil the space-time interpretation presented here, as those are not effectively described by the emergent metric in general.

[2]If the correction term $\delta\alpha$ is truncated at the linear order in δx, the scalar curvature becomes $R = \frac{9M}{r_0^3}$. However, it should be regarded as negligible for $r_0 \simeq 2M$ and $L \ll r_0$, because it is much smaller than the typical curvature of the system $R \simeq \frac{9}{2r_0^2} \ll \frac{1}{L^2}$. Thus, it is consistent with the Schwarzschild solution. The higher-order correction terms are much smaller than the linear-order correction, in $-L < \delta x^i < L$, for example, and the curvature is exactly zero by taking them into consideration.

small x dependence in $\alpha_i(x)$, the wave function can be estimated by using the WKB approximation, and $\delta\alpha_i(x)$ gives only higher-order corrections. In particular, we are mainly interested in the direction of the propagation, which can be read off only from the local structure of the geometry. For that purpose, we can even focus on a much smaller region around each points inside the Weyl semimetal. Thus, α_i can be approximated by a constant to study the direction at each point, even in inhomogeneous Weyl semimetals which can resemble both sides of the horizon.

Another way to see a relation to the black hole is an explicit construction of light cones. A null vector n^μ satisfies $n^\mu n^\nu g_{\mu\nu} = 0$, which is

$$[1-(\alpha_i)^2](n^0)^2 + 2n^0 n^i\alpha_i - (n^i)^2 = 0. \tag{9}$$

Consider a radial null vector which should be the most efficient if one wants to escape from the black hole, namely, $n^i \propto \alpha_i$, then we have $(n^i\alpha_i)^2 = (n^i)^2(\alpha_j)^2$. With this, we can solve the null condition as

$$\frac{n^i\alpha_i}{n^0} = (\alpha_i)^2 \pm \sqrt{(\alpha_i)^2}, \tag{10}$$

which is always positive for $(\alpha_i)^2 > 1$. This means that the light propagation is always in a certain direction. It passes through the surfaces $\alpha_i x^i = \text{const}$, which correspond to $r = \text{const}$ surfaces in the Schwarzschild metric, only from one side to the other but never goes back, which happens also inside a "black hole." See Fig. 1 for a pictorial view of the light-cone structure.

Note that the event horizon of black holes is defined as the boundary of the causal past of the future null infinity and depends on the global structure of the geometry. Since the type-II Weyl semimetal mimics only the local geometry of the black hole, the interpretation depends on how it is embedded in the global geometry of black holes. There could be some other interpretation of the effective metric (3), depending on the embedding. For example, (3) can be also viewed as a local metric in an ergoregion of a Kerr geometry.

III. GENERIC BOUNDARY CONDITIONS FOR TYPE-II WEYL SEMIMETALS

Following Ref. [12], here we obtain the most generic boundary conditions for the type-II Weyl semimetals in the continuum limit.[3] For the type-II Weyl material, we introduce a single flat boundary surface at $x^3 = 0$, with a generic boundary condition

$$N\psi(x^3 = 0) = 0, \tag{11}$$

where N is a constant complex 2×2 matrix. With the Hamiltonian (1), the Hermiticity condition for the system requires

$$\psi_1^\dagger(\sigma_3 + \alpha_3\mathbf{1})\psi_2 = 0 \tag{12}$$

for arbitrary wave functions ψ_1 and ψ_2 at the boundary. We like to find the most generic N which leads to (12). First, noting $\det N = 0$ from (11), we can write N as

$$N = \begin{pmatrix} 1 & \beta \\ \gamma & \gamma\beta \end{pmatrix}, \tag{13}$$

up to the overall normalization of N [which is irrelevant to the boundary condition (11)], so the solution of (11) is written as $\psi_i = (-\beta, 1)^T f_i$ with a scalar function f_i. Then, the condition (12) is recast to

$$|\beta|^2 - 1 + \alpha_3(|\beta|^2 + 1) = 0. \tag{14}$$

So, we find that a consistent boundary condition exists only when $|\alpha_3| < 1$ and $|\beta| = \sqrt{\frac{1-\alpha_3}{1+\alpha_3}}$. In other words, the most general boundary condition for Weyl semimetals with the Hamiltonian (1) is

$$\left(1, \sqrt{\frac{1-\alpha_3}{1+\alpha_3}}e^{i\theta}\right)\psi(x^3 = 0) = 0 \tag{15}$$

with a boundary condition parameter θ ($0 \leqslant \theta < 2\pi$).

Note that introduction of the boundary at $x^3 = 0$ does not allow $|\alpha_3| > 1$. This also implies that the vector α of type-II Weyl semimetals cannot be normal to the boundary.[4] Of course, setting $\alpha_3 = 0$ brings us back to the generic boundary condition studied in Ref. [12].

IV. EDGE DISPERSION OF TYPE-II WEYL SEMIMETALS

The edge state should exist as a result of the topological protection since the bulk-edge correspondence [2–4] works also for the type-II Weyl semimetals [6,13]. The edge state is localized at the boundary because of the imaginary part of the momentum normal to the boundary. (Note that without any addition of a Hamiltonian at the boundary, just the bulk Hamiltonian provides the edge states due to the existence of the boundary.) Although the bulk mode satisfies the boundary condition by taking an appropriate linear combination of the incoming and outgoing modes at the boundary, such a linear combination cannot be taken for the edge mode since only one of these two modes corresponds to the edge mode and the other is an unphysical non-normalizable mode. Thus, the boundary condition gives an additional condition to the momenta of the edge mode.

Let us solve the Hamiltonian eigenequation $H\psi = E_{\text{edge}}\psi$ for the edge states, by imposing the most generic boundary condition (15). It is quite straightforward and we show only the result here. The energy eigenvalue is

$$E_{\text{edge}} = \alpha_1 p_1 + \alpha_2 p_2 - \sqrt{1-\alpha_3^2}(p_1\cos\theta - p_2\sin\theta). \tag{16}$$

The edge-state wave function is

$$\psi = \begin{pmatrix} -\sqrt{\frac{1-\alpha_3}{1+\alpha_3}}e^{i\theta} \\ 1 \end{pmatrix} \exp[ik_3x^3] \tag{17}$$

[3] See also Refs. [24–26] for 1D and 2D generic boundary conditions.

[4] This bound was independently studied in Ref. [23]. The authors would like to thank Zyuzin for bringing Ref. [23] to our attention.

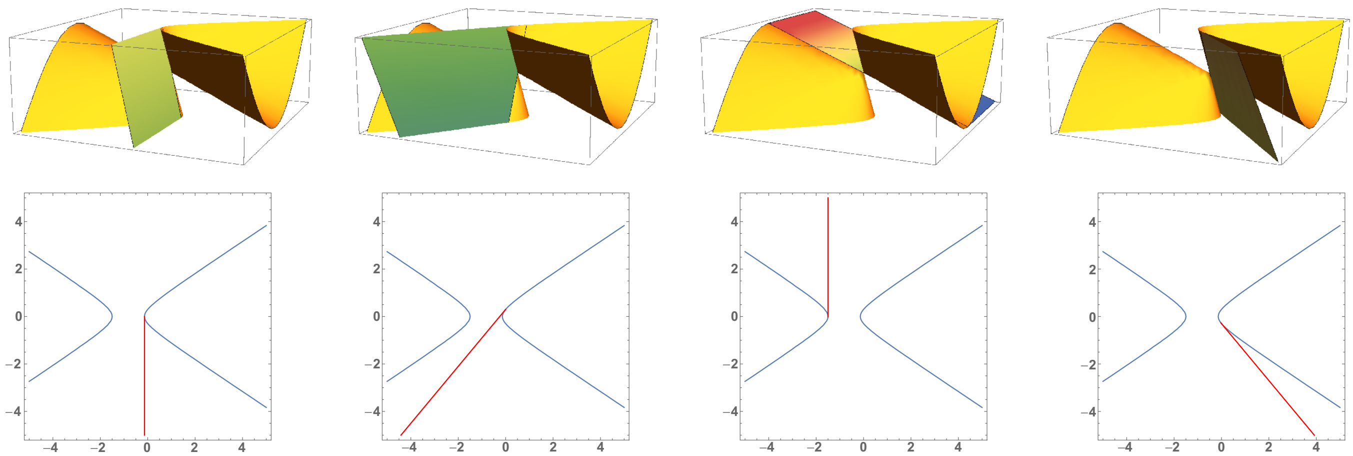

FIG. 2. Upper row: Energy dispersion E_{bulk} as a function of p_1 and p_2 at the slice $p_3 = \mathrm{Re}[k_3]$, and the edge dispersion E_{edge} given in (16) with (19). We chose $\alpha_2 = \alpha_3 = 0$ with $\alpha_1 = -1.2$ (type II), and the boundary condition parameter s$\theta = 0$, $\theta = \pi/2$, $\theta = \pi$, and $\theta = (3\pi/2)$ (from left to right). The edge dispersion is always flat, and tangential to the bulk-edge dispersion. Lower row: Corresponding slices at $E = 0.3$, shown in the (p_1, p_2) plane. Blue curved lines are for the bulk dispersion, and red half-lines are for the edge dispersion.

with the complex momentum k_3:

$$k_3 \equiv \frac{\alpha_3(p_1\cos\theta - p_2\sin\theta) - i(p_1\sin\theta + p_2\cos\theta)}{\sqrt{1-\alpha_3^2}}. \quad (18)$$

The imaginary part of k_3 shows the localization of the edge state at the boundary. As the wave function decays exponentially away from the boundary, the particle is localized at the boundary. The wave function for $x^3 \neq 0$ describes the penetration to the inside of the material due to the quantum uncertainty. When the material exits in the region $x^3 \geqslant 0$, the normalizability condition for the wave function is $\beta \equiv \mathrm{Im}[k_3] > 0$, which is equivalent to

$$p_1 \sin\theta + p_2\cos\theta < 0. \quad (19)$$

There also exists the real part of k_3, which would have been absent if $\alpha_3 = 0$. It provides an oscillatory wave function localized near the surface. When $\alpha_3 = 0$, the wave function is oscillating only in the direction tangential to the boundary and the phase does not change in the normal direction. However, when $\alpha_3 \neq 0$, there exists the oscillatory wave function in the x^3 direction, which implies that the direction of the constant phase is no longer orthogonal to the boundary.

The edge dispersion is a straight line in the (p_1, p_2) plane at the constant energy slice. We show some of the examples of the edge and bulk dispersions in Fig. 2. Note that the bulk dispersion is a two-dimensional surface but the edge dispersion is a one-dimensional line in the three-dimensional momentum space of (p_1, p_2, p_3). Figure 2 shows the plots on the slice at $p_3 = \mathrm{Re}[k_3]$ in the three-dimensional momentum space, where the edge dispersion extends.

It should be emphasized that the edge dispersion does not intersect with the bulk dispersion. The same Hamiltonian is shared by both the bulk modes and the edge modes, and both dispersion relations are given by the same expression $g^{\mu\nu}k_\mu k_\nu = 0$. The edge dispersion always lies outside the bulk dispersion since the dispersion relation in terms of the metric $g^{\mu\nu}k_\mu k_\nu = 0$ simply gives $g^{\mu\nu}p_\mu p_\nu = 0$ for the bulk mode while $g^{\mu\nu}p_\mu p_\nu = \beta^2$ for the edge mode, but the edge and bulk dispersions merge at the single merging point $\beta = 0$. (The exception is the $E = 0$ slice at which the edge dispersion could overlap with the bulk one, for some special values of θ.)

One interesting observation is that the edge dispersion is always tangential to the bulk dispersion. The next section is devoted for a proof that the edge dispersion is always tangential to the bulk dispersion at the merging point.

V. TANGENTIALITY THEOREM OF EDGE AND BULK DISPERSIONS

In this section, we show that any edge dispersion is tangential to the bulk dispersion at the merging point. The statement was explicitly made by Haldane [14] for generic Weyl semimetals and here we provide a proof of it. This theorem is not only for the type-II Weyl semimetals, but applicable to any bulk and edge state which satisfies the definitions that we will provide below.

We first consider the generic bulk mode. It is a propagating mode in the bulk of materials, and so the wave function of it is given in terms of the momenta

$$\psi \sim e^{ip_i x^i - iEt}, \quad (20)$$

where p_i is the spatial momenta and E is the energy. For stable states, the energy E has to be real. The momenta p_i should also be real for the normalizability of the state. Thus, we assume that both p_i and E are real.

The edge mode is a localized mode around the surface boundary of the material. It satisfies the same equation of motion but the momentum normal to the boundary has an imaginary part

$$\psi \sim e^{ip_i x^i - \beta z - iEt}, \quad (21)$$

where z is the normal direction to the boundary and β is the imaginary part of the momentum in the direction. Thus, the wave function is suppressed away from the boundary.

The surface boundary condition needs to be imposed on the wave functions above at the boundary. For bulk modes, it can be satisfied by taking an appropriate superposition of the incoming mode $p_z < 0$ and the outgoing mode $p_z > 0$. On the other hand, for the edge modes, these two modes would correspond to those with opposite signs of β. The linear combination cannot be taken due to the normalizability condition and, thus, the boundary condition gives an additional constraint on the momenta. This structure is generic, and the edge dispersion is subject to additional constraints in general. The additional constraints, however, play no important role in the proof.

The statement of the theorem which we prove is as follows. Bulk and edge modes are tangential to each other at their merging point, for any system which satisfies the following conditions:

(i) Bulk mode is defined as the states whose momenta are real.

(ii) For the edge mode, only one of the momenta has an imaginary part.

(iii) The energy is given by a function of momenta. The function is holomorphic and the form is shared for bulk and edge modes.

(iv) The energy may not be real for arbitrary complex values of momenta, but is real for bulk modes and edge modes.

Here, we provide a proof. According to the assumptions, both the bulk and edge dispersions are given by subspaces of the curve

$$E = F(k_i), \tag{22}$$

where k_i are momenta, which are complex in general. The bulk dispersion is the subspace of the curve in which all the momenta are real,

$$E = F(p_i), \tag{23}$$

where p_i are real momenta. The edge dispersion is given in terms of the same function F as[5]

$$E = F(p_{i(\neq z)}, p_z + i\beta), \tag{24}$$

but the momenta satisfy additional constraints which come from the boundary condition. If the edge dispersion continues to $\beta = 0$, it is merged into the bulk dispersion there.

Now, it is straightforward to show that the edge dispersion is tangential to the bulk dispersion. The tangent space of the bulk dispersion is given by

$$0 = dE = \sum_i \frac{\partial F}{\partial p_i} dp_i. \tag{25}$$

On the other hand, the tangent space of the edge dispersion is expressed as

$$0 = dE = \sum_{i(\neq z)} \frac{\partial F}{\partial p_i} dp_i + \frac{\partial F}{\partial p_z}(dp_z + i d\beta). \tag{26}$$

The Hermiticity condition for the bulk mode implies that all $\frac{\partial F}{\partial p_i}$ must be real since all real momenta p_i are independent for the bulk mode. Then, the real and imaginary parts of (26) give

$$0 = dE = \sum_i \frac{\partial F}{\partial p_i} dp_i, \tag{27}$$

$$0 = \frac{\partial F}{\partial p_z}, \tag{28}$$

respectively. At the merging point $\beta = 0$, the first equation agrees with the tangent space of the bulk dispersion there. Therefore, the edge dispersion is tangent to the bulk dispersion at the merging point. The imaginary part (28) must be satisfied on the merging point, for the energy of the edge mode to be real.

Finally, we emphasize again that the above proof is valid for any system, for example, a system on a discrete lattice, as long as it satisfies the conditions (i)–(iv) above, though in this paper we focus on the continuum limit in the type-II Weyl semimetals. For the case of type-II Weyl semimetals, it can be seen in Fig. 2 that the edge dispersion is tangential to the bulk dispersion.

VI. ESCAPE FROM BLACK HOLES

Let us study the propagation direction of the edge state to see whether it can escape from the black hole. The propagating direction is given by the tangent vector to the world line of the particle $n^\mu \propto \frac{dx^\mu}{d\tau}$, where τ is a proper time on the world line. The relation between the propagation direction n^μ and the four-momentum p_μ for the world line is $n^\mu = g^{\mu\nu} p_\nu$. Here, the edge modes have the same effective metric as the bulk modes have since the same condition $g^{\mu\nu} k_\mu k_\nu = 0$ is shared by both the bulk and edge dispersions. However, this does not mean that the edge modes cannot escape from the black hole. In general, edge modes have dispersion relations which are quite different from the light cone of massless particles in vacuum. Even in the case of $\alpha_i = 0$, which should be identified with the case of the flat space, this applies. The edge dispersion of our case can be obtained by putting the edge modes for the flat space onto the geometry with the effective metric which is the same as that of the bulk modes. As the edge modes on the flat space do not look like the particle propagation in vacuum, those on the effective metric do not resemble any particle propagation around (inside) the real black holes. Thus, the edge modes possibly may be able to escape from the black hole, as we will demonstrate explicitly below.

Substituting the edge dispersion (16) and $p_3 = \mathrm{Re}[k_3]$, we find

$$n^0 = \frac{1}{\sqrt{1-\alpha_3^2}}(p_1 \cos\theta - p_2 \sin\theta), \tag{29}$$

$$n^1 = -p_1 + \frac{\alpha_1}{\sqrt{1-\alpha_3^2}}(p_1 \cos\theta - p_2 \sin\theta), \tag{30}$$

$$n^2 = -p_2 + \frac{\alpha_2}{\sqrt{1-\alpha_3^2}}(p_1 \cos\theta - p_2 \sin\theta), \tag{31}$$

$$n^3 = 0. \tag{32}$$

[5]It is because the same Hamiltonian is shared by both the bulk and edge modes. In fact, the bulk dispersion relation (2) reduces to the edge dispersion relation (16) when we substitute the complex momentum k_3 given in (18) of the edge mode to p_3 of the bulk relation (2).

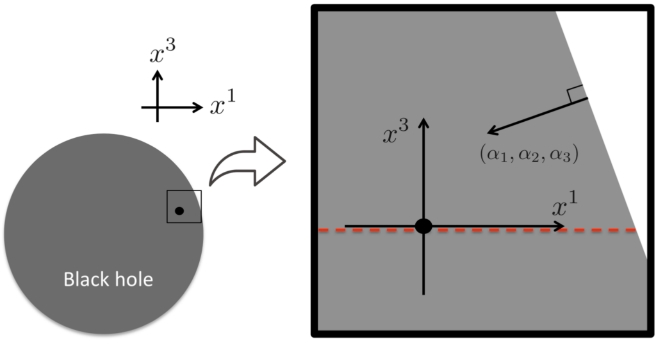

FIG. 3. The surface we introduce (the red dashed line) is at $x^3 = 0$. Since the horizon is perpendicular to the vector α_i, any edge mode propagating in the positive-x^1 direction on the surface $x^3 = 0$ can escape the Schwarzschild black hole.

Note that automatically we obtained $n^3 = 0$, which is consistent with the fact that the edge mode is localized on the boundary, since the condition $n^3 = 0$ implies that it propagates only along the boundary $x^3 = 0$. Thus, the effective metric to which the edge mode is subject is an induced metric on $x^3 = 0$. In fact, the same result is obtained by using the induced metric $h_{\mu\nu}$, namely, $n^\mu = g^{\mu\nu} p_\nu = h^{\mu\nu} p_\nu$ for the edge modes.

The expression above applies to any α_1 and α_2. The type-II Weyl semimetal has $\alpha_1^2 + \alpha_2^2 > 1 - \alpha_3^2$. Without loss of generality, we can take $\alpha_1 < -\sqrt{1-\alpha_3^2}$ and $\alpha_2 = 0$, by using the rotation in the (x^1, x^2) plane. So let us concentrate on this case. All the bulk modes propagate in the direction given by the vector α_i, as explained in Sec. II. For $\alpha_1 < -\sqrt{1-\alpha_3^2}$ and $\alpha_2 = 0$, bulk modes can move only in the direction toward larger values of $\alpha_i x^i$, while the direction toward the horizon is $\alpha_i dx^i < 0$. We are in the black hole. Now, consider the edge mode living on the surface defined by $x^3 = 0$. On the surface, as $dx^3 = 0$, the direction toward the horizon (for escaping from the black hole) is $\alpha_1 dx^1 < 0$, namely, the positive direction of x^1. See Fig. 3 for the space-time allocation of the system in the black hole. So, if we can find an edge mode which propagates in the positive direction of x^1, that is $\frac{dx^1}{dt} = n^1/n^0 > 0$, it is traveling toward the horizon. Although we cannot see the behavior at the horizon away from the system, we extrapolate it assuming that similar condition continues to the horizon, and we conclude that the edge mode can escape from the black hole. In other words, for (p_1, p_2) satisfying (19) and $E_{\text{edge}} > 0$ with (16), if there exists (p_1, p_2) giving $n^1/n^0 > 0$, the edge mode can move toward the event horizon, implying that it can escape from the black hole, eventually. As we will see below, the answer depends on the parameter θ of the boundary condition.

In order to see whether the edge mode can escape from the black hole, it is convenient to rewrite n^0 and n^1 in terms of energy E_{edge};

$$n^0 = \frac{E_{\text{edge}} - \alpha_1 p_1}{1-\alpha_3^2}, \tag{33}$$

$$n^1 = \frac{\alpha_1}{1-\alpha_3^2} E_{\text{edge}} + \frac{1-\alpha_1^2-\alpha_3^2}{1-\alpha_3^2} p_1. \tag{34}$$

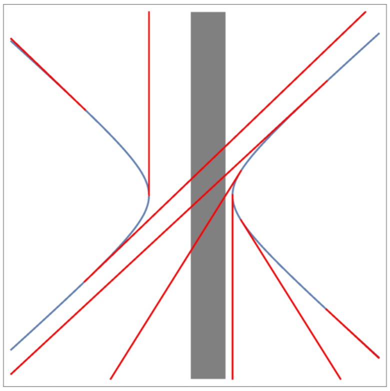

FIG. 4. Edge dispersion (red line) on $E_{\text{edge}} = \text{const}$ surface. The parameters are taken as $\alpha_1 = -1.2$ and $\alpha_2 = \alpha_3 = 0$. The boundary condition parameter θ is $\theta = \frac{9}{8}\pi, \theta = \pi, \theta = \frac{7}{8}\pi, \theta = \frac{3}{4}\pi, \theta = \frac{1}{2}\pi$, $\theta = 0$, $\theta = \frac{3}{2}\pi$, and $\theta = \frac{5}{4}\pi$, from upper left to lower right. The shaded region (40) lies between the hyperboloid of the bulk dispersion (blue line).

Here, we consider only the edge modes with positive energy $E_{\text{edge}} > 0$, and the other parameters satisfy $\alpha_1 < -\sqrt{1-\alpha_3^2}$ and $-1 < \alpha_3 < 1$. The sign of n^0 depends on given energy E_{edge} and momentum p_1 as

$$n^0 > 0 \quad \text{for} \quad p_1 > \alpha_1^{-1} E_{\text{edge}}, \tag{35}$$

$$n^0 < 0 \quad \text{for} \quad p_1 < \alpha_1^{-1} E_{\text{edge}}, \tag{36}$$

while the sign of n^1 flips as

$$n^1 > 0 \quad \text{for} \quad p_1 < -\frac{\alpha_1}{1-\alpha_1^2-\alpha_3^2} E_{\text{edge}}, \tag{37}$$

$$n^1 < 0 \quad \text{for} \quad p_1 > -\frac{\alpha_1}{1-\alpha_1^2-\alpha_3^2} E_{\text{edge}}, \tag{38}$$

where both $\alpha_1^{-1} E_{\text{edge}}$ and $-\frac{\alpha_1}{1-\alpha_1^2-\alpha_3^2} E_{\text{edge}}$ are negative. From the conditions $E_{\text{edge}} > 0, \alpha_1 < -\sqrt{1-\alpha_3^2}$, and $-1 < \alpha_3 < 1$, it is straightforward to obtain the following relation;

$$-\frac{\alpha_1}{1-\alpha_1^2-\alpha_3^2} E_{\text{edge}} < \alpha_1^{-1} E_{\text{edge}}. \tag{39}$$

Thus, there is always a range of momentum p_1:

$$-\frac{\alpha_1}{1-\alpha_1^2-\alpha_3^2} E_{\text{edge}} < p_1 < \alpha_1^{-1} E_{\text{edge}}, \tag{40}$$

which shows $n^1/n^0 > 0$ or, equivalently, a possible edge mode escaping away from the black hole.

However, note that it does not immediately mean that there exists such an edge mode which can escape from the black hole. This edge mode needs a value of p_1 which is in the range (40), that is, the edge dispersion needs to allow p_1 to overlap with (40). This can be seen in Fig. 4: The edge dispersions for various values of θ are shown pictorially in Fig. 4, for the case of $\alpha_1 = -1.2$ and $\alpha_2 = \alpha_3 = 0$. If the edge dispersion (colored in red) intersects with the range (40) (the gray region), then that is the edge mode escaping away from the black hole.

To obtain an analytic expression for the boundary condition parameter θ to allow such an edge mode escaping away from

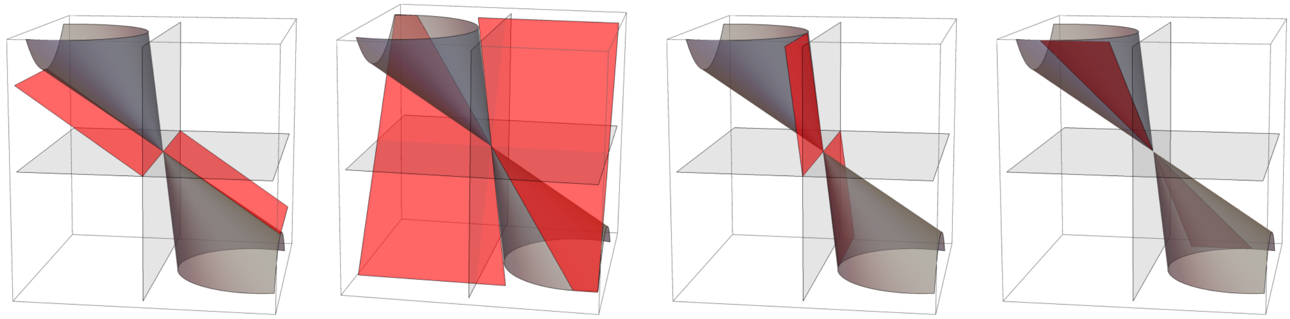

FIG. 5. Space-time picture of the bulk (gray) and edge (red) modes. The horizontal directions are x^1 and x^2, while the vertical direction is time. We chose $\alpha_2 = \alpha_3 = 0$ with $\alpha_1 = -1.2$ (type II), and the boundary condition parameters $\theta = 0, \theta = \pi/2, \theta = \pi$, and $\theta = (3\pi/2)$ (from left to right).

the black hole, we classify the edge dispersion by a class of ranges of θ, as follows.

(i) For $\theta = 0$, the edge dispersion is given by

$$E_{\text{edge}} = \left(\alpha_1 - \sqrt{1-\alpha_3^2}\right)p_1. \tag{41}$$

Since the momentum is fixed for given E_{edge} and satisfies $0 > p_1 > \alpha_1^{-1}E_{\text{edge}}$, the edge mode cannot escape from the black hole.

(ii) For $0 < \theta < \cos^{-1}(\alpha_1^{-1}\sqrt{1-\alpha_3^2}) < \pi$, the edge dispersion has $p_2 > 0$ at the merging point $\beta = \text{Im}k_3 = 0$, and the condition $\beta > 0$ gives the upper bound of p_1 but no lower bound. Since the edge dispersion is a straight line with $p_1 > \alpha_1^{-1}E_{\text{edge}}$ at the merging point, the edge dispersion extends to the region (40). Thus, the edge mode can escape from the black hole.

(iii) For $\theta = \cos^{-1}(\alpha_1^{-1}\sqrt{1-\alpha_3^2}) < \pi$, the edge mode is on the asymptote of the hyperboloid of the bulk mode. There is no upper or lower bound on p_1, and the edge dispersion extends to the region (40). The edge mode can escape from the black hole.

(iv) For $\cos^{-1}(\alpha_1^{-1}\sqrt{1-\alpha_3^2}) < \theta < \pi$, the edge dispersion has $p_2 < 0$ at the merging point $\beta = \text{Im}k_3 = 0$, and the condition $\beta > 0$ gives the lower bound of p_1 but no upper bound. Since the edge dispersion is a straight line with $p_1 < -\frac{\alpha_1}{1-\alpha_1^2-\alpha_3^2}E_{\text{edge}}$ at the merging point, the edge dispersion extends to the region (40). Thus, the edge mode can escape from the black hole.

(v) For $\theta = \pi$, the edge dispersion is given by

$$E_{\text{edge}} = \left(\alpha_1 + \sqrt{1-\alpha_3^2}\right)p_1. \tag{42}$$

Since the momentum is fixed for given E_{edge} and satisfies $p_1 < -\frac{\alpha_1}{1-\alpha_1^2-\alpha_3^2}E_{\text{edge}}$, the edge mode cannot escape from the black hole.

(vi) For $\pi < \theta < \cos^{-1}(\alpha_1^{-1}\sqrt{1-\alpha_3^2})$, the edge dispersion has $p_2 > 0$ at the merging point $\beta = \text{Im}k_3 = 0$, and the condition $\beta > 0$ gives the upper bound of p_1. Since the edge dispersion is a straight line with $p_1 < -\frac{\alpha_1}{1-\alpha_1^2-\alpha_3^2}E_{\text{edge}}$ at the merging point, which has maximum of p_1, the edge mode cannot escape from the black hole.

(vii) For $\theta = \cos^{-1}(\alpha_1^{-1}\sqrt{1-\alpha_3^2}) > \pi$, no edge mode is allowed near the Weyl point. The bulk dispersion is approximately given by a hyperboloid. The merging point of edge and bulk modes is in $p_1 \to \pm\infty$, and the edge dispersion extends outward from the merging point.

(viii) For $\cos^{-1}(\alpha_1^{-1}\sqrt{1-\alpha_3^2}) < \theta < 2\pi$, the edge dispersion has $p_2 < 0$ at the merging point $\beta = \text{Im}k_3 = 0$, and the condition $\beta > 0$ gives the lower bound of p_1. Since the edge dispersion is a straight line with $p_1 > \alpha_1^{-1}E_{\text{edge}}$ at the merging point, which has minimum of p_1, the edge mode cannot escape from the black hole.

In summary, in the convention $\alpha_1 < -\sqrt{1-\alpha_3^2}$ and $\alpha_2 = 0$, the edge mode can escape away from the black hole, when the boundary condition parameter θ satisfies

$$0 < \theta < \pi\ . \tag{43}$$

In Fig. 5, we plot the space-time structure of the bulk mode and the edge mode, for various values of θ. It shows possible directions (and velocities) in space for the modes to move along. It confirms the result (43).

This (43) means that for a randomly chosen consistent boundary condition θ, it may allow the edge modes propagating out of the black hole defined by the bulk mode of the type-II Weyl semimetals. Therefore, in building a black hole analog by the type-II Weyl semimetals, one needs to carefully choose the surface boundary conditions of the material, such that the edge modes do not violate the causality produced by the black hole.

Let us elaborate more on the reason for this conclusion. The effective metric (3) is determined by the bulk excitations, so the light-cone structure is fixed by it. The edge modes generically propagate outside of the light cone, so *edge modes are tachyonic*. The edge dispersion can be expressed in the form

$$g^{\mu\nu}p_\mu p_\nu = -\beta^2, \tag{44}$$

where the effective metric is the same with that for the bulk dispersion. Thus, the edge modes behave as tachyons whose imaginary mass comes from the imaginary part of k_3. Note that the overall structure of the edge dispersion in the momentum space does not take the standard form of tachyons since the effective imaginary mass β also depends on momenta. With a proper choice of the boundary condition, they can even propagate in the direction opposite to the bulk tilted light cone. Therefore, the edge modes can eventually go outside the black hole horizon.

VII. SUMMARY

In this paper, we have studied generic boundary conditions and generic edge dispersions in type-II Weyl semimetals in the continuum and the low-energy limits. Based on the bulk dispersion argument [5] that type-II Weyl semimetals can be regarded as the inside of a black hole, we have explored the possibility of having an edge mode which can escape away from the black hole horizon. We have found that the generic boundary condition is parametrized by a single rotation parameter θ $(0 \leqslant \theta < 2\pi)$ as (15), and for a part of the range of the parameter $(0 < \theta < \pi$ for $\alpha_2 = 0)$ there exists an edge mode escaping away from the black hole.

For a realization of the black hole by the type-II Weyl semimetals, since any material has its surface, we need a special care about the choice of the boundary condition. Our analysis shows that θ needs to be in the range $\pi \leqslant \theta \leqslant 2\pi$ not to violate the black hole causal structure. A safe way is to choose, for example, $\theta = 3\pi/2$ which amounts to the boundary condition

$$\left(1, -i\sqrt{\frac{1-\alpha_3}{1+\alpha_3}}\right)\psi(x^3 = 0) = 0 \tag{45}$$

for the Hamiltonian (1) and the spatial coordinate $x^3 \geqslant 0$ for the material with the surface at $x^3 = 0$. Since the edge modes are absent in the real black holes, the type-II Weyl semimetals always have extra modes which do not resemble any particles around the black hole. The condition above is chosen such that the extra modes do not take the information from inside to outside. It might be possible in some cases that another condition may be useful to distinguish the edge modes from the others. The boundary condition should be tuned on demand.

In this paper we have dealt only with the continuum limit of the type-II Weyl semimetals because it has enabled us to study the most generic boundary conditions, which are necessary for checking the possibility of escaping from the black hole. The physical realization of the specific value of θ depends on discrete lattice models of the type-II Weyl semimetal. Once the bulk discrete model is obtained, one takes the continuum limit and extracts the value of θ from the numerically observed edge-mode dispersion (16), then one can check whether the edge mode is escaping out of the black hole or not.

Note that our study here based on the local structure of the geometry does not entirely certify that our condition lets the edge mode escape out of the horizon since the event horizon is defined by the global structure of the geometry. As seen in Fig. 3, the black hole horizon is located away from the point at which we study the direction of the propagation of the edge mode. The condition we study in this paper is the one for edge modes to propagate toward the horizon in the spatial slice. If one wants to describe whether the edge mode can pass the horizon or not, one needs more detailed analyses of how one joins the type-II Weyl semimetal with a type-I Weyl semimetal at the horizon, meaning a spatially dependent $\alpha_i(x)$. Approaches to introduce spatially dependent $\alpha_i(x)$ by using inhomogeneous Weyl semimetals are studied elsewhere [5,7–11]. It is straightforward to introduce the spatial dependence by introducing small inhomogeneity, which would simply give spatial dependence in $\alpha_i(x)$ at the lowest-order approximation. More precise analyses on the spatial dependence is beyond the scope of this paper.

The identification of the Weyl semimetals with the black hole can be extended to topological "insulators." It is known that regarding one of the momenta of Weyl semimetals to be a nonzero constant reduces the system to a topological insulator. The type-I Weyl semimetal with $p_i = m$ is a two-dimensional topological insulator of class A, and we can consider the same dimensional reduction from the type-II Weyl semimetal to a topological "insulator," which is not insulating due to the tilted light cone. Our analysis is valid even with putting $p_2 = m$. So, black hole validity can be checked in the same manner, with the boundary condition parameter θ.

The important part of the analyses in this paper is the most generic boundary conditions in the continuum limit. The idea of the method was used [15] to find a topological charge of the edge state, which results in the discovery of states localized at corners [16,17] (which were recently called corner states or hinge states in higher-order topological insulators [18,19]). It would be interesting to explore the edge-mode contributions to the black hole interpretation of various deformed topological insulators, as well as type-III and -IV Weyl semimetals [20]. With these deformations of the Weyl semimetal Hamiltonians, D-brane interpretation of the bands [21] may not persist, that is also an interesting issue.

Although the propagation of the bulk modes mimics that in a black hole geometry, whether the Hawking radiation emanating from the event horizon (which is the boundary between type-I and -II semimetals [22]) exists or not is rather a subtle question, as the Hawking radiation originates in the change of the quantum vacua in black hole formation. It is challenging to construct a theoretical framework of Weyl semimetals accompanying a Hawking temperature and possible experimental set-ups.[6]

Introducing a surface boundary to the type-II Weyl semimetals in turn means slicing a black hole, which sounds impossible in general relativity. Black holes in brane world scenario would be the closest example in particle physics, and we hope our condensed-matter analyses may inspire also particle physics in the future.

ACKNOWLEDGMENTS

We would like to thank D. R. Candido, H. Katsura, M. Koshino, M. Kurkov, M. Ochi, R. Okugawa, and A. Zyuzin for valuable comments. This work is supported in part by JSPS KAKENHI Grant No. JP17H06462.

[6]For related studies, see Refs. [9,10,27–30].

[1] N. P. Armitage, E. J. Mele, and A. Vishwanath, Rev. Mod. Phys. **90**, 015001 (2018).
[2] R. Jackiw and C. Rebbi, Phys. Rev. D **13**, 3398 (1976).
[3] Y. Hatsugai, Phys. Rev. Lett. **71**, 3697 (1993).
[4] X.-G. Wen, *Quantum Field Theory of Many-body Systems: From the Origin of Sound to an Origin of Light and Electrons* (Oxford University Press, Oxford, 2004).
[5] G. Volovik and K. Zhang, J. Low Temp. Phys. **189**, 276 (2017).
[6] A. A. Soluyanov, D. Gresch, Z. Wang, Q. Wu, M. Troyer, X. Dai, and B. A. Bernevig, Nature (London) **527**, 495 (2015).
[7] G. E. Volovik, JETP Lett. **104**, 645 (2016).
[8] S. Guan, Z.-M. Yu, Y. Liu, G.-B. Liu, L. Dong, Y. Lu, Y. Yao, and S. A. Yang, npj Quantum Mater. **2**, 23 (2017).
[9] H. Huang, K.-H. Jin, and F. Liu, Phys. Rev. B **98**, 121110(R) (2018).
[10] H. Liu, J.-T. Sun, H. Huang, F. Liu, and S. Meng, arXiv:1809.00479.
[11] L. Liang and T. Ojanen, Phys. Rev. Res. **1**, 032006 (2019).
[12] K. Hashimoto, T. Kimura, and X. Wu, PTEP **2017**, 053I01 (2017) [Erratum: PTEP **2019**, 029201 (2019)].
[13] T. M. McCormick, I. Kimchi, and N. Trivedi, Phys. Rev. B **95**, 075133 (2017).
[14] F. Haldane, arXiv:1401.0529.
[15] K. Hashimoto and T. Kimura, Phys. Rev. B **93**, 195166 (2016).
[16] K. Hashimoto, X. Wu, and T. Kimura, Phys. Rev. B **95**, 165443 (2017).
[17] K. Hashimoto, X. Wu, and T. Kimura, " Edge-of-edge states," Presentation at TMS Intensive-Interactive Meeting, https://drive.google.com/file/d/0B4lWuy3Pyd6IM050RlZHT0pLMmc/view.
[18] W. A. Benalcazar, B. A. Bernevig, and T. L. Hughes, Science **357**, 61 (2017).
[19] F. Schindler, A. M. Cook, M. G. Vergniory, Z. Wang, S. S. Parkin, B. A. Bernevig, and T. Neupert, Sci. Adv. **4**, eaat0346 (2018).
[20] J. Nissinen and G. E. Volovik, JETP Lett. **105**, 447 (2017).
[21] K. Hashimoto and T. Kimura, PTEP **2016**, 013B04 (2016).
[22] G. E. Volovik, Phys. Usp. **61**, 89 (2018).
[23] A. A. Zyuzin and A. Y. Zyuzin, Phys. Rev. B **97**, 041203(R) (2018).
[24] M. Tanhayi Ahari, G. Ortiz, and B. Seradjeh, Am. J. Phys. **84**, 858 (2016).
[25] M. Kharitonov, J.-B. Mayer, and E. M. Hankiewicz, Phys. Rev. Lett. **119**, 266402 (2017).
[26] D. R. Candido, M. Kharitonov, J. C. Egues, and E. M. Hankiewicz, Phys. Rev. B **98**, 161111(R) (2018).
[27] M. Zubkov, Mod. Phys. Lett. A **33**, 1850047 (2018).
[28] G. Liu, L. Jin, X. Dai, G. Chen, and X. Zhang, Phys. Rev. B **98**, 075157 (2018).
[29] M. Zubkov, Universe **4**, 135 (2018).
[30] Y.-G. Chen, X. Luo, F.-Y. Li, B. Chen, and Y. Yu, Phys. Rev. B **101**, 035130 (2020).